

**Figure 2.** Plot of heat capacity at constant pressure,  $C_p$ , as a function of temperature. The inset shows an expanded view of the low-temperature heat capacity effect.

phase transition with two  $C_p$  peaks at 111.4 and 112.0 K and a higher order phase transition with two  $C_p$  peaks at 185.8 and 191.3 K. It is very interesting that the temperature of the 111–112 K phase transition occurs at the temperature where the first Mössbauer spectrum change occurs. The higher order phase transition can be seen to evolve over a large temperature range with  $C_p$  peaks at the temperature where the Mössbauer spectrum becomes a single average doublet.

It is suggested that the lower temperature phase transition is an order–disorder phase transition. At temperatures below this first phase transition the triangular complexes each have a static distortion reflecting the iron valence states. One iron is  $\text{Fe}^{\text{II}}$  and the other two are  $\text{Fe}^{\text{III}}$ . These distorted complexes are ordered in domains, e.g., homogeneous regions of crystallite where the distortions of the  $\text{Fe}_3\text{O}$  units are ordered in the same sense. At the low-temperature phase transition these domains disappear and the sense of distortion becomes randomly distributed throughout the crystallite. Cooperativity is the essence of a phase transition. The packing arrangement in **1** involves stacks of pyridine ligands with an interplanar separation of  $c/3 = 3.5 \text{ \AA}$ . The pyridine ligands from neighboring molecules experience appreciable  $\pi$ – $\pi$  overlap and this could lead to cooperativity and the first-order phase transition at 111–112 K. In a later paper<sup>8</sup> it will be shown that the third doublet that appears in the Mössbauer spectrum (see Figure 1) at  $\sim 117 \text{ K}$  is attributable to  $\text{Fe}_3\text{O}$  complexes that are electronically delocalized. The first-order phase transition at  $\sim 112 \text{ K}$  leads to a change in the potential energy diagram such that above this temperature the zero point energies of the delocalized and localized complexes become comparable in magnitude.

The higher temperature phase transition is not first order, for it evolves over an extensive temperature range. It is likely that this phase transition involves  $\text{Fe}_3\text{O}$  molecules becoming thermally activated to change their sense of distortion combined eventually with the pyridine solvate molecules starting to rotate about the  $C_3$  axes of the stacks of  $\text{Fe}_3\text{O}$  molecules. Preliminary single-crystal X-ray diffraction work<sup>6</sup> indicates that the  $C_3$  axis disappears at  $\sim 190 \text{ K}$  as the crystal is cooled from 300 K.

Definitive evidence for the motion of solvate molecules in the solid state has been determined for compound **2**,  $[\text{Fe}_3\text{O}(\text{O}_2\text{CCH}_3)_6(4\text{-CH}_3\text{-py})_3](\text{C}_6\text{D}_6)$ , where the solvate molecule is a deuterated benzene. Compound **2** is isostructural with **1** and shows a similar temperature dependence in its Mössbauer spectrum. A complete single-crystal  $^2\text{H}$  NMR study has been carried out on **2** at room temperature. Rotations were carried out about three orthogonal axes. At every setting of the single crystal only a single quadrupole-split doublet is seen. It is clear that the  $\text{C}_6\text{D}_6$

molecule is rapidly rotating about a 6-fold axis to make all deuterium sites equivalent. The principal components of the deuterium quadrupole interaction tensor were found to be  $-13.5 \pm 0.5$ ,  $-18.3 \pm 0.5$ , and  $+31.6 \pm 0.5 \text{ kHz}$ . These values are considerably reduced from what is expected for a  $\text{C}_6\text{D}_6$  fixed in the solid in which case the axially symmetric principal components are  $-67$  and  $135 \text{ kHz}$ . Reorientation about the  $C_3$  axis along the molecular stacks or about a  $C_2$  axis perpendicular to it is also present in addition to the rotation about the 6-fold axis.

Variable-temperature IR studies of **1**, isostructural  $[\text{Fe}_2^{\text{III}}\text{Co}^{\text{II}}\text{O}(\text{O}_2\text{CCH}_3)_6(\text{py})_3](\text{py})$ , and symmetric  $[\text{Fe}^{\text{III}}_3\text{O}(\text{O}_2\text{CCH}_3)_6(\text{py})_3]\text{ClO}_4$  clearly indicate, based on the  $\text{M}_3\text{O}$  asymmetric stretch regions, that compound **1** is "valence localized" in terms of the IR experiment in the 500–800- $\text{cm}^{-1}$  region. Thus, **1** and the  $\text{Fe}^{\text{III}}_2\text{Co}^{\text{II}}$  complex each show two asymmetric stretches, whereas, the higher symmetry  $\text{Fe}^{\text{III}}_3$  complex exhibits one such band. This same conclusion was reached by Cannon et al.<sup>9</sup> At or above the higher temperature phase transition, the pyridine solvate molecules are rotating and the  $\text{Fe}_3\text{O}$  molecules are changing their sense of distortion much faster than can be sensed by the Mössbauer technique but slower than would average the two  $\text{Fe}_3\text{O}$  asymmetric stretching bands.

Dynamics in the solid state involving the onset of motion in a ligand, solvate molecule, or counterion at a certain temperature could in general be major factors determining whether the intramolecular electron transfer in a given mixed-valence complex is fast or slow. We have also detected phase transitions for the mixed-valence complex  $[\text{Fe}_3\text{O}(\text{O}_2\text{CCH}_3)_6(3\text{-CH}_3\text{-py})_3](3\text{-CH}_3\text{-py})$ ,<sup>10</sup> which has a different solid-state structure than **1**, and for mixed-valence biferrocenium triiodide.<sup>11</sup>

**Acknowledgment.** We thank the National Institutes of Health for support of the work at the University of Illinois through Grant HL13652 to D.N.H. and the National Science Foundation (P. C.M. 8118912 to R.J.W.) for the work at the University of Louisville.

(9) Cannon, R. D.; Montri, L.; Brown, D. B.; Marshall, K. M.; Elliott, C. M. *J. Am. Chem. Soc.* **1984**, *106*, 2591.

(10) Sorai, M.; Shiomi, Y.; Hendrickson, D. N.; Oh, S. M., unpublished results.

(11) Sorai, M.; Hendrickson, D. N.; Dong, T.-Y.; Cohn, M. J., unpublished results.

### Stereoselective Synthesis of $\gamma,\delta$ -Epoxy- $\beta$ -methyl- $\gamma$ -(trimethylsilyl)alkanols. Synthesis of the C(1)–C(7) Segment of 6-Deoxyerythronolide B

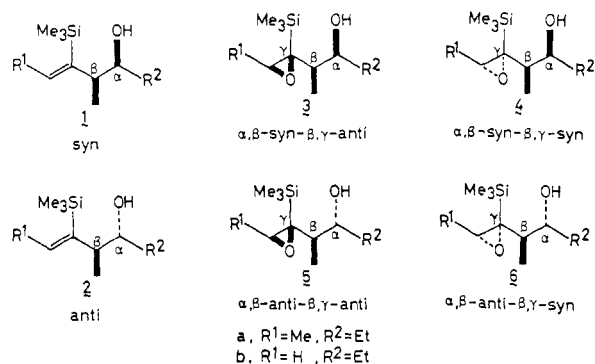
Yuichi Kobayashi, Hiroshi Uchiyama, Hiroshi Kanbara, and Fumie Sato\*

Department of Chemical Engineering  
Tokyo Institute of Technology  
Meguro, Tokyo 152, Japan

Received April 8, 1985

Previously, we have reported a highly enantio- and diastereoselective synthesis of *syn*- and *anti*- $\beta$ -methyl- $\gamma$ -(trimethylsilyl) homoallyl alcohols **1** and **2**.<sup>1</sup> In connection with ongoing program directed toward the utilization of these alcohols for synthesis of naturally occurring acyclic molecules such as macrolide and ionophore antibiotics, we have been interested in stereoselective synthesis of four possible diastereoisomers of  $\gamma,\delta$ -epoxy- $\beta$ -

(1) (a) Sato, F.; Kusakabe, M.; Kobayashi, Y. *J. Chem. Soc., Chem. Commun.* **1984**, 1130. (b) Kobayashi, Y.; Kitano, Y.; Sato, F. *Ibid.* **1984**, 1329. (c) Sato, F.; Kusakabe, M.; Kato, T.; Kobayashi, Y. *Ibid.* **1984**, 1331.

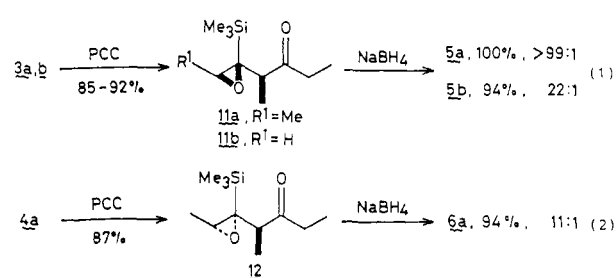


methyl- $\gamma$ -(trimethylsilyl)alkanols **3–6** from **1** and/or **2** by relative asymmetric induction from the preexisting chiral centers. We report here our successful approach to **3–6** and the application of the reaction products to the synthesis of the C(1)–C(7) portion of 6-deoxyerythronolide B.

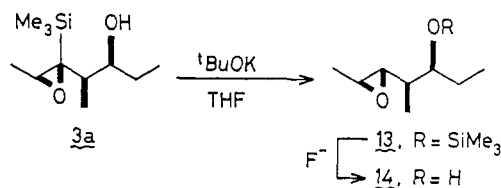
First, the direct epoxidation of **1** and **2** was studied by using TBHP/VO(acac)<sub>2</sub> and mCPBA.<sup>2,3</sup> The results summarized in Table I indicate that the reaction proceeded stereoselectively to afford the  $\beta,\gamma$ -anti<sup>4</sup> isomers (**3** and **5**) as major products. Especially, the epoxidation of **1** with TBHP proceeded with near 100% selectivity to provide **3** exclusively (entries 1 and 3) as observed in the case of allyl alcohols having a trimethylsilyl group on the double bond.<sup>5</sup> The presence of SiMe<sub>3</sub> is indispensable to get high selectivity in this epoxidation, since the TBHP epoxidation of *syn*-(*E*)-4-methyl-5-hepten-3-ol, prepared by protodesilylation of **1a**,<sup>6</sup> afforded a mixture of the *syn* and *anti* epoxides in a ratio of 3:2. Next, epoxidation of the esters of **1** and **2** with mCPBA was examined, and it was found that the major products were the  $\beta,\gamma$ -*syn* isomers (entries 6–8 in Table I). Among them, epoxidation of the benzoate of **1a** proceeded with synthetically useful stereoselectivity of 6:1, thus allowing preparation of **4** predominantly.

Since we could not prepared **5** and **6** highly selectively by direct epoxidation of **2**, we turned our attention to synthesizing them via an indirect method. Based on our previous findings,<sup>1a</sup> we considered that a metal hydride reduction of the epoxy ketones **11** and **12** derived from **3** and **4**, respectively, would proceed with high diastereoselectivity owing to the steric bulk of SiMe<sub>3</sub>, to afford the corresponding "Cram" products and it turned out to be the case. Thus, reduction of **11** and **12** with NaBH<sub>4</sub> in MeOH at –10 °C proceeded with >11:1 selectivity to provide the corresponding alcohols **5** and **6** (eq 1 and 2).

The epoxides **3–6** thus prepared were readily converted to the corresponding silyl ethers via a 1,4-SiMe<sub>3</sub> group shift under the reaction conditions that are effective for the 1,4-SiMe<sub>3</sub> group shift of  $\gamma$ -SiMe<sub>3</sub> homoallyl alcohols.<sup>1a</sup> Thus, reaction of **3a** with *t*-



BuOK in THF (0 °C, 5 min) gave rise to the silyl ether **13** in 90% yield, which was converted to the free epoxy alcohol **14** by treatment with *n*-Bu<sub>4</sub>NF.



In the remaining paragraph, we will describe the synthesis of the optically active C(1)–C(7) segment **19** of 6-deoxyerythronolide B, lankanolide, and oleandronolide, where the results mentioned above are effectively used for controlling the relative stereochemistry (Scheme 1).<sup>7</sup> The optically active starting material **15** (>95% ee) was prepared according to the procedure published earlier from our laboratory<sup>1b</sup> starting with (2*S*,3*S*)-*trans*-crotyl epoxy alcohol (>95% ee)<sup>8</sup> and (*Z*)-[(trimethylsilyl)propenyl]-magnesium bromide prepared by the hydromagnesiation<sup>9</sup> reaction of 1-(trimethylsilyl)-1-propyne (four steps, 53% overall yield from the epoxy alcohol). Reaction of **15** with the lithium enolate of BHT propionate<sup>10</sup> followed by reduction and protection afforded **16** exclusively.<sup>1c</sup> Epoxidation of **16** with TBHP and subsequent treatment with *t*-BuOK gave **17** as a sole product: no diastereoisomer of **17** could be detected by <sup>1</sup>H and <sup>13</sup>C NMR spectroscopy. The epoxide **17** was then converted exclusively into **18** by reaction with [1-(trimethylsilyl)vinyl]magnesium bromide (0 °C, 10 days) followed by treatment with *n*-Bu<sub>4</sub>NF.<sup>11</sup> Finally **18** was transformed into **19** by the sequence of simple reactions. The stereochemistry of **19** was confirmed by conversion to the known compound **20**,<sup>7f</sup> whose <sup>1</sup>H and <sup>13</sup>C NMR spectra and the optical rotation ([ $\alpha$ ]<sub>D</sub><sup>25</sup> –3.8° (*c* 1.00, CHCl<sub>3</sub>)) were fully identical in

(2) For reviews, see: Sharpless, K. B.; Verhoeven, T. R. *Aldrichimica Acta* **1979**, *12*, 63. Bartlett, P. A. *Tetrahedron* **1980**, *36*, 2. Rao, A. S.; Paknikar, S. K.; Kirtane, J. G. *Ibid.* **1983**, *39*, 2323.

(3) Stereoselective epoxidation of acyclic homoallyl alcohols, see: Mihelich, E. D.; Daniels, K.; Eickhoff, D. J. *J. Am. Chem. Soc.* **1981**, *103*, 7690. Schmid, G.; Fukuyama, T.; Akasaka, K.; Kishi, Y. *Ibid.* **1979**, *101*, 259. Johnson, M. R.; Kishi, Y. *Tetrahedron Lett.* **1979**, 4347. Williams, D. R.; Grote, J.; Harigaya, Y. *Ibid.* **1984**, *25*, 5231. Other examples of epoxidation of homoallyl alcohols, see: Yamamoto, Y.; Yatagai, H.; Maruyama, K. *J. Am. Chem. Soc.* **1981**, *103*, 3229. Beau, J.-M.; Aburaki, S.; Pougny, J.-R.; Sinay, P. *Ibid.* **1983**, *105*, 621. Kozlowski, A. P.; Schmiesing, R. J.; Sorgi, K. L. *Tetrahedron Lett.* **1981**, *22*, 2059. Hiyama, T.; Kimura, K.; Nozaki, H. *Ibid.* **1981**, *22*, 1037. Coxon, J. M.; Simpson, G. W.; Steel, P. J.; Trenerry, V. C. *Ibid.* **1983**, *24*, 1427. Indirect method for preparation of epoxides from homoallyl alcohols, see: Bartlett, P. A.; Jernstedt, K. K. *J. Am. Chem. Soc.* **1977**, *99*, 4829.

(4) The stereoconfiguration was classified as "syn" and "anti" according to the definition of Masamune: Masamune, S.; Ali, S. A.; Snitman, D. L.; Garvey, D. S. *Angew. Chem., Int. Ed. Engl.* **1980**, *19*, 557. Masamune, S.; Kaiho, T.; Garvey, D. S. *J. Am. Chem. Soc.* **1982**, *104*, 5521.

(5) Hasan, I.; Kishi, Y. *Tetrahedron Lett.* **1980**, *21*, 4229. Tomioka, H.; Suzuki, T.; Oshima, K.; Nozaki, H. *Ibid.* **1982**, *23*, 3387. Narula, A. S. *Ibid.* **1982**, *23*, 5579.

(6) Sato, F.; Tanaka, Y.; Sato, M. *J. Chem. Soc., Chem. Commun.* **1983**, 165.

(7) Recent publications in this area, see: (a) Masamune, S.; Hiram, M.; Mori, S.; Asrof, Sk.; Garvey, D. S. *J. Am. Chem. Soc.* **1981**, *103*, 1568. (b) Danishefsky, S.; Kato, N.; Askin, D.; Kerwin, J. F., Jr. *Ibid.* **1982**, *104*, 360. (c) Stork, G.; Paterson, I.; Lee, F. K. C. *Ibid.* **1982**, *104*, 4686. (d) Vedejs, E.; Dolphin, J. M.; Mastalerz, H. *Ibid.* **1983**, *105*, 127. (e) Kinoshita, M.; Ohsawa, N.; Gomi, S. *Carbohydr. Res.* **1982**, *109*, 5. (f) Paterson, I. *Tetrahedron Lett.* **1983**, *24*, 1311. (g) Paterson, I.; Patel, S. K.; Porter, J. R. *Ibid.* **1983**, *24*, 3395. (h) Oikawa, Y.; Nishi, T.; Yonemitsu, O. *Ibid.* **1983**, *24*, 3635.

(8) Rossiter, B. E.; Katsuki, T.; Sharpless, K. B. *J. Am. Chem. Soc.* **1981**, *103*, 464.

(9) Sato, F.; Ishikawa, H.; Sato, M. *Tetrahedron Lett.* **1981**, *22*, 85.

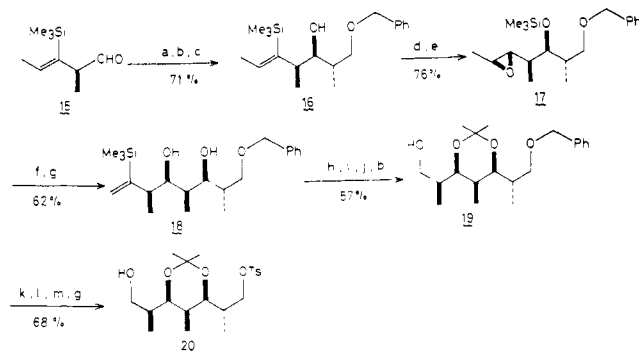
(10) Heathcock, C. H.; Pirrung, M. C.; Montgomery, S. H.; Lampe, J. *Tetrahedron* **1981**, *37*, 4087.

(11) Nakata, M.; Takao, H.; Ikeyama, Y.; Sakai, T.; Tatsuta, K.; Kinoshita, M. *Bull. Chem. Soc. Jpn.* **1981**, *54*, 1749. Nakata, M.; Enari, H.; Kinoshita, M. *Ibid.* **1982**, *55*, 3283. Nakata, T.; Fukui, M.; Ohtsuka, H.; Oishi, T. *Tetrahedron* **1984**, *40*, 2225. Corey, E. J.; Hase, T. *Tetrahedron Lett.* **1979**, 335. Hungerbühler, E.; Seebach, D. *Angew. Chem., Int. Ed. Engl.* **1979**, *18*, 958. Wood, R. D.; Ganem, B. *Tetrahedron Lett.* **1982**, *23*, 707. Johnson, M. R.; Nakata, T.; Kishi, Y. *Ibid.* **1979**, 4343. Nagaoka, H.; Kishi, Y. *Tetrahedron* **1981**, *37*, 3873. Mori, K.; Iwasawa, H. *Ibid.* **1980**, *36*, 87. Lipshutz, B. H.; Kozlowski, J. A. *Ibid.* **1984**, *49*, 1147. Ho, P.-T. *Can. J. Chem.* **1982**, *60*, 90. Inanaga, J.; Kawanami, Y.; Yamaguchi, M. *Chem. Lett.* **1981**, 1415. Corey, E. J.; Trybulski, E. J.; Melvin, L. S., Jr.; Nicolaou, K. C.; Secrist, J. A.; Lett, R.; Sheldrake, P. W.; Falck, J. R.; Brunelle, D. J.; Haslanger, M. F.; Kim, S.; Yoo, S. *J. Am. Chem. Soc.* **1978**, *100*, 4618. Helbig, W. *Ann. Chem.* **1984**, 1165. Roush, W. R.; Adam, M. A.; Peseckis, S. M. *Tetrahedron Lett.* **1983**, *24*, 1377. Suzuki, T.; Samito, H.; Tomioka, H.; Oshima, K.; Nozaki, H. *Ibid.* **1982**, *23*, 3597. Pfaltz, A.; Mattenberger, A. *Angew. Chem., Int. Ed. Engl.* **1982**, *21*, 71.

Table I. Epoxidation of Homoallyl Alcohols and Their Esters

entry	substrate <sup>a</sup>	reagent	yield, %	major product <sup>b</sup>	selectivity <sup>c</sup>
1		TBHP <sup>d</sup>	88		>99:1
2	1a	mCPBA <sup>e</sup>	90	3a	4:1
3		TBHP <sup>d</sup>	91		>99:1
4 <sup>f</sup>	1b	TBHP <sup>d</sup>	91	3b	2:1
5 <sup>f</sup>	2a	mCPBA <sup>e</sup>	88	5a	3:1
6		mCPBA <sup>e</sup>	96		6:1
7		mCPBA <sup>e</sup>	100		5:1
8 <sup>g</sup>	8	mCPBA <sup>e</sup>	89	10	3:1

<sup>a</sup> Diastereoisomerically homogeneous (>99% pure) racemic substrates were used for each reaction. <sup>b</sup> The stereochemistry of the epoxides was unambiguously established (see supplementary data). <sup>c</sup> Determined by <sup>1</sup>H and <sup>13</sup>C NMR spectroscopy. <sup>d</sup> The reaction was carried out using TBHP in CH<sub>2</sub>Cl<sub>2</sub> at 0 °C. <sup>e</sup> The reaction was carried out by using mCPBA in CH<sub>2</sub>Cl<sub>2</sub> at 0 °C → room temperature. <sup>f</sup> The anti alcohol 2b gave a mixture of 5b and 4b in a ratio of 2:1. <sup>g</sup> The corresponding acetate gave a similar result.

Scheme 1<sup>a</sup>

<sup>a</sup> (a) CH<sub>3</sub>CH<sub>2</sub>COOBHT, LDA; (b) LiAlH<sub>4</sub>; (c) PhCH<sub>2</sub>Br, NaH; (d) TBHP, VO(acac)<sub>2</sub>; (e) *t*-BuOK, THF; (f) CH<sub>2</sub>=C(SiMe<sub>3</sub>)MgBr, CuI, THF; (g) *n*-Bu<sub>4</sub>NF; (h) KH, HMPA; (i) Me<sub>2</sub>C(OMe)<sub>2</sub>, PPTS, CH<sub>2</sub>Cl<sub>2</sub>; (j) O<sub>3</sub>, MeOH; (k) TBSCl, DMAP; (l) H<sub>2</sub>, Pd/C; (m) TsCl, C<sub>5</sub>H<sub>5</sub>N.

all respects with data kindly provided by I. Paterson.

**Acknowledgment.** We are grateful to Dr. Ian Paterson of University Chemical Laboratory, England, for providing us data (<sup>1</sup>H and <sup>13</sup>C NMR and [α]<sub>D</sub>) of 20.

**Supplementary Material Available:** Assignment of the stereochemistry of the epoxides prepared in text and listing of optical rotations and spectral data (8 pages). Ordering information is given on any current masthead page.

Chemistry and Structure of the First 10-Sb-3 Species<sup>1</sup>

Constantine A. Stewart, Richard L. Harlow, and Anthony J. Arduengo III\*

Contribution No. 3778, Central Research & Development Department, Experimental Station E. I. du Pont de Nemours & Company  
Wilmington, Delaware 19898

Received May 17, 1985

We report the chemistry and structure of 5-aza-2,8-dioxo-3,7-di-*tert*-butyl-1-stibabicyclo[3.3.0]octa-3,6-diene (ADSbO). ADSbO is the first molecule to contain the 10-Sb-3 bonding system. In spite of the large size of the antimony center, 10-Sb-3 ADSbO exhibits a planar geometry analogous to the previously reported 10-P-3 and 10-As-3 systems.<sup>2,3</sup> The formation of 10-Sb-3 ADSbO is in stark contrast to the formation of a 20-Bi-9 system when the central atom is a bismuth.<sup>4</sup>

As with the similar phosphorus and arsenic systems, ADSbO shows no evidence for the presence of the 8-Sb-3 electromorph;<sup>3</sup> however, there is a marked thermochromism at the melting point (116 °C). Solid 10-Sb-3 is a light yellow-green color which turns dark red on melting and back to yellow-green on freezing. Solutions of ADSbO are red in color with the intensity dependent upon temperature and solvent polarity. The solution and solid-state <sup>13</sup>C NMR spectra of ADSbO are identical and consistent with the 10-Sb-3 structure.<sup>5</sup> The <sup>1</sup>H NMR (CD<sub>2</sub>Cl<sub>2</sub>) exhibits resonances at δ 1.39 (s, 18 H) and 8.46 (s, 2 H). The ring proton resonance at δ 8.46 confirms the trend observed earlier in the ADPO and ADAso systems.<sup>3</sup> This observation suggests the importance of positive charge delocalization in the ligand backbone and discounts ring current effects for these 10-Pn-3 systems.

ADSbO is prepared by a route analogous to the previously reported 10-Pn-3 systems.<sup>2,3</sup> While ADSbO is thermally stable it is sensitive to both water and oxygen. The structure (Figure 1) of ADSbO was verified by single-crystal X-ray diffraction. Table I gives the bond lengths and angles in ADSbO. It is interesting to note the Sb-O and Sb-N bonds in ADSbO are 17 and 22 pm longer than the corresponding bonds in ADAso. This correlates well with the 20-pm increase in covalent radius on going from arsenic to antimony. The central pnictogen-nitrogen bond is increasing at a faster rate than the pnictogen-oxygen bond as one goes down the family from phosphorus to antimony. This is consistent with a bonding scheme which forces the stabilization of the pnictogen lone pairs at the 10-Pn-3 center by mixing more s character into the lone pair orbitals. This results in decreased s participation in the Pn-N bond. Thus this bond is lengthened.

Another consequence of the larger atomic radius is the extension of the pnictogen center out of the ligand mandible. This extension can be seen in the decrease of the O-Pn-O bond angles of the ADPnO series. This results in the availability of a large antimony surface in ADSbO.

(1) The *N-X-L* system has previously been described (Perkins, C. W.; Martin, J. C.; Arduengo, A. J., III; Lau, W.; Alegria, A.; Kochi, J. K. *J. Am. Chem. Soc.*, **1980**, *102*, 7753). *N* valence electrons about a central atom X, with *L* ligands.

(2) Culley, S. A.; Arduengo, A. J., III. *J. Am. Chem. Soc.* **1984**, *106*, 1164.

(3) Culley, S. A.; Arduengo, A. J., III. *J. Am. Chem. Soc.* **1985**, *107*, 1089.

(4) Stewart, C. A.; Calabrese, J. C.; Arduengo, A. J., III. *J. Am. Chem. Soc.* **1985**, *107*, 3397.

(5) <sup>13</sup>C{<sup>1</sup>H} NMR spectra of 10-Sb-3 ADSbO consists of the following resonances: δ 28.8 (CH<sub>3</sub>), 38.0 (C(CH<sub>3</sub>)), 117.8 (CH), 176.7 (CO). The solid-state <sup>13</sup>C NMR spectra was analogous to the solution spectrum. <sup>17</sup>O δ 305; <sup>15</sup>N δ -90 (<sup>17</sup>O and <sup>15</sup>N spectra relative to H<sub>2</sub><sup>17</sup>O and NH<sub>4</sub><sup>15</sup>NO<sub>3</sub>, respectively). All solution NMR spectra were run in CD<sub>2</sub>Cl<sub>2</sub>, satisfactory analysis (CHN) were obtained for ADSbO.

(6) This perspective drawing was made with the KANVAS computer graphics program. This program is based on the program SCHAKAL of E. Keller (Kristallographisches Institute der Universität Freiburg, FRG), which was modified by A. J. Arduengo, III (E. I. du Pont de Nemours & Co., Wilmington, DE) to produce the back and shadowed planes. The planes bear 50-pm grids and the lighting source is at infinity so that the shadow size is meaningful.